

Dependence of the Melting Temperature on Pressure up to 2000 Bar in Uranium Dioxide, Tungsten, and Graphite¹

M. Musella,² C. Ronchi,^{2,3} and M. Sheindlin⁴

The melting points of uranium dioxide, tungsten, and graphite were measured as a function of the isostatic pressure up to 2000 bar (200 MPa), in a laser-heated autoclave filled with inert gas. The measured melting curves and their slopes were compared with predictions obtained from the Clausius–Clapeyron equation and existing thermochemical data of these substances. While for tungsten and graphite the results show reasonable agreement with the equilibrium thermodynamic calculations, the melting point of UO₂ increases with pressure with a slope more than three times larger than expected.

KEY WORDS: graphite; high pressure; laser pulse; melting point; tungsten; uranium dioxide.

1. INTRODUCTION

The dependence of the melting point of materials on pressure defines an important invariant curve in the phase diagram, which is a function of the chemical and physical properties of both the solid and the liquid. For this reason, when an equation of state is formulated for a given liquid, the correct reproduction of the experimental melting curve represents one of the main requirements for the model. In the context of the INTAS Project 93-0066, dealing with the equation of state of uranium dioxide up to the

¹ Paper presented at the Fifth International Workshop on Subsecond Thermophysics, June 16–19, 1998, Aix-en-Provence, France.

² European Commission, Joint Research Centre, European Institute for Transuranium Elements, Postfach 2340, D-76010 Karlsruhe, Germany.

³ To whom correspondence should be addressed.

⁴ Russian Academy of Sciences, IVTAN, Moscow, Russia.

critical point, the variation of the melting point of this compound was investigated in the pressure range up to 2000 bar (200 MPa).

Measurement of the melting point of high-melting materials under high-pressure conditions is subject to strong limitations. In fact, under high compression conditions, both static and dynamic direct temperature measurements are very difficult if not impossible. However, in view of measuring the average slope of the melting curve, dT_m/dp , the broad range of pressures, which can be now produced in laboratory experiments, compensates, in part, for the low precision of the melting point determination. Thus, for a large number of substances, the melting curve has been determined up to several kilobars, from measurements where the experimental accuracy of the temperature is very poor (see, e.g., Ref. 1). For this reason, in the lower pressure range (up to a few kilobars), the melting curve parameters, in particular its slope, remain in most cases rather imprecise.

The measurements reported in this paper have been obtained with a technique which enables the melting temperature to be determined with an accuracy of a few kelvins, under isostatic pressure conditions up to approximately 2 kbar. Furthermore, errors in the evaluation of the melting point variation due to absolute calibration of the pyrometer (including emissivity and absorption uncertainties) are avoided by performing the measurements at different pressures under the same, clean conditions. Comparative experiments were performed on UO_2 in the form of a standard nuclear reactor fuel pellet and on two other materials: tungsten, for which the published data on high-pressure melting are rather discordant, and graphite, a material whose melting point is still a matter of controversy.

2. EXPERIMENTAL

Laser surface heating is the only applicable technique to obtain controlled melting under containerless conditions in materials with poor or strongly temperature-dependent electrical conductivity.

The experimental setup (see schematic in Fig. 1) consists of a gas-filled autoclave with a single window at the top. The sample is mounted in the middle of the autoclave and is heated above the melting point by a pulsed Nd-YAG laser beam impinging on its upper surface, whose temperature is measured by a fast two-channel spectral pyrometer. The wavelength windows were fixed at 650 and 550 nm. The brightness temperatures measured in the two channels were independently converted into real temperature by using the measured emissivities. The 650-nm signal was normally considered as the most reliable, the second one being regarded as only a corroborating measurement. The pyrometer sensor is a silicon

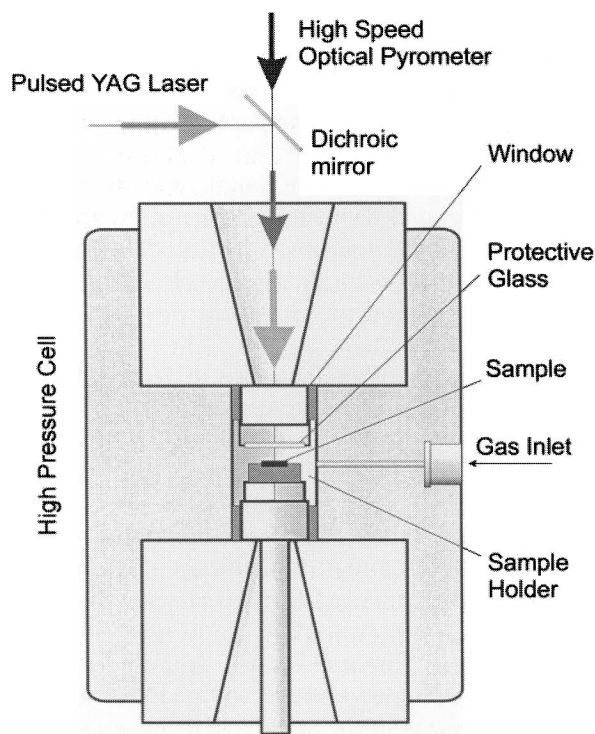


Fig. 1. Schematic of the experimental setup.

photodiode whose signal is amplified through a logarithmic amplifier and subsequently treated by an analog/digital converter; the response time is $< 10 \mu\text{s}$. The features of the instrument and the calibration procedure are described in Ref. 2. The temperature of thermal arrest during the sample cool-down determines the melting point. The melting "plateau" was normally of a few milliseconds' duration, a time interval during which several hundred pyrometric measurements were performed. This made it possible to examine in detail the undercooling and recalescence stage and, hence, to assign a precise value to the freezing temperature.

Though the schematic of the experiment is simple, a number of difficulties has been resolved in order to obtain the necessary accuracy in the temperature range from 3000 to 5000 K; three of them were particularly crucial.

The first concerns the temperature homogeneity on the surface. A pronounced radial temperature profile across the laser spot may produce both systematic and random variations of the measured brightness temperature,

which are larger than the investigated effects. Only the use of a high-quality laser beam with a large diameter (5 mm) and an effective flat power profile (<5% radial variation) made it possible to spot with the pyrometer an area of 0.3-mm diameter where the temperature was sufficiently homogeneous during the experiment.

The applied (“rectangular”) pulse length was of the order of 10 to 30 ms, whereby the integrated deposited power (a few joules) was selected in order to exceed the melting point by a few hundred kelvins, with a temperature increase rate on the sample surface of the order of $10^6 \text{ K} \cdot \text{s}^{-1}$. The power and pulse duration were selected in view of obtaining a melting thickness of approximately 0.1 mm.

In graphite (and, at low pressures, also in UO_2), the sublimation or vaporization of the sample during the pulse in the gas environment lead to the rapid formation of soot in the *vicinity* of the surface. The experiment shows that—probably due to gas convection—the soot concentration increases with the distance from the central axis of the laser beam. Oblique pyrometric measurements present, therefore, the double inconvenience of a less precise spectral emissivity and of a significant gray absorption from the soot particles. In our case, the axis of the pyrometer (reflected by a semi-transparent mirror) coincides with that of the laser beam, so that the conditions are in this respect optimal, and, in addition, during heat-up, the optical path of the pyrometer was completely cleared from soot particles.

Finally, refraction effects in the autoclave from the heated layer of the gas near the sample surface were sufficiently reduced only by placing the sample at a close distance (a few millimeters) from the window glass. Several checks with different materials showed that the disturbance of gas (both He and Ar) on pyrometric temperature measurements was eventually negligible over the explored pressure range.

2.1. Samples

The samples used were platelets 4 to 9 mm in size, so that the produced molten pool of approximately 3-mm diameter and 20- to 100- μm thickness—depending on the material—was flat and sufficiently stable in shape during the pulse. Since the same sample was used for several pulses at different pressures, tests were conducted by varying the laser pulse parameters in order to establish the conditions under which the molten mass features were best reproducible at all pressures. After a sequence of shots at high pressures, a melting point determination at 100 bar was normally repeated, confirming that no emissivity changes occurred. This check was, however, not possible for graphite, since this material undergoes a pronounced structural transformation on melting.

2.1.1. Uranium Dioxide

The material used was a sintered pellet (95% of the theoretical density) of UO_2 of technical purity, according to the nuclear fuel standard. The peak temperature was fixed at approximately 3500 K, in order to preserve during the pulse the initial stoichiometry ($\text{O}/\text{M} = 2.002 \pm 2$); in fact, up to this temperature, chemical reduction could be prevented by the traces of oxygen (~ 100 ppm O_2) present in the inert gas of the autoclave. Even after subsequent pulses at increasing pressures, the molten pool was observed to maintain a regular, flat shape. Figure 2 shows a scanning electron micrograph of the sample after a typical experiment. The refrozen zone shows a regular network of cracks of isotropic orientation, indicating that the freezing process proceeded homogeneously, in the absence of large radial temperature gradients.

The normal spectral emissivity, $\epsilon_{650 \text{ nm}} = 0.85$, used for the calculation of the true temperature, was taken from experimental measurements [3].

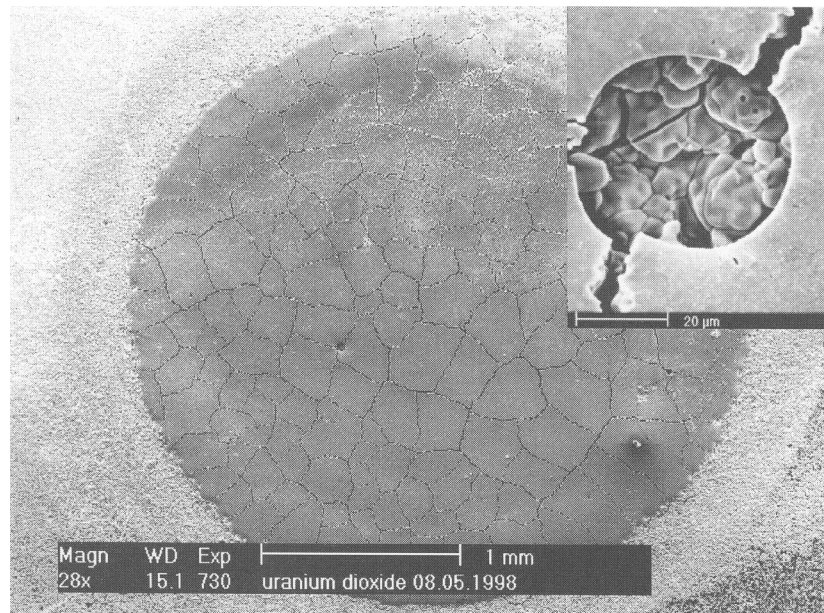


Fig. 2. View of the melted zone in an UO_2 sample. The pyrometer field aperture was a central spot of 0.3-mm diameter. In the inset, where the small dark hole in the center is enlarged, it can be seen that the refrozen layer is detached from the bulk. For this reason, in laser-pulse experiments liquid movements can uncover cooler areas affecting the measurements of the freezing point. In our case freezing was homogeneous.

2.1.2. Tungsten

The samples were laminated foils of 0.1-mm thickness, produced by Plansee. Preliminary melting experiments at room pressures indicated that the normal spectral emissivity, $\epsilon_{650\text{ nm}}$, of the "as-fabricated" material was somewhat higher than that previously measured on specimens prepared from electrochemically polished small rods (0.40 against 0.36) [4]. Actually, only after repeated melting did the measured emissivity decrease to the expected value of 0.36. This effect is, therefore, likely due to the lamination texture of the foil or to the presence of oxide impurities on the surface.

2.1.3. Graphite

Graphite was of the RW1 Ringsdorff type; it is a low-density ($1550\text{ kg}\cdot\text{m}^{-3}$) material, highly resistant to thermal shocks and possessing optimal wetting properties with respect to liquid carbon. The latter property, in conjunction with the almost perfectly homogeneous laser heating, enabled—to our knowledge, for the first time—a compact, large molten pool to be produced on the surface of the sample. The refrozen material has a complex structure, consisting of an internal columnar layer, grown upon the solid substrate, and an external layer formed by small platelets parallel to the sample surface. It should be noted that the fast freezing of these external platelets sufficiently defines, in size and shape, the contour of the liquid volume. The observed surface of the frozen mass is regular and perfectly dense, so that no large disturbances in emissivity are expected on freezing. Finally, the porosity measured inside the frozen zone provides a good estimation of the expansion on melting. Since, however, fabricated RW1 graphite is very porous, this conclusion was corroborated by the results of melting experiments on highly oriented pyrolytic graphite, whose density is close to the crystal theoretical density. The metallography analysis indicates in the two types of graphite an equal, large expansion on melting, of the order of 45% of the solid volume.

3. RESULTS

3.1. Uranium Dioxide

The melting point of UO_2 was previously measured in a low-pressure vessel with two windows. In this vessel a two-stage pulse could be applied: the sample was heated by a continuous-wave laser at the conditioning temperature of approximately 3100 K. A pulse was then applied, raising the temperature to a peak value of approximately 3500 K (Fig. 3). As expected

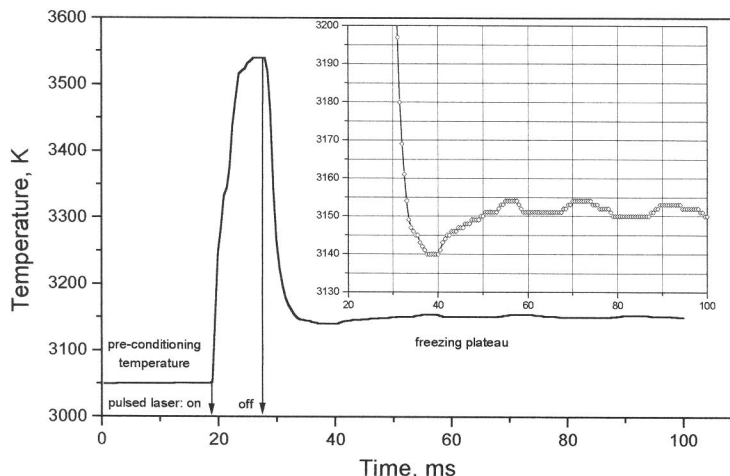


Fig. 3. Recorded thermogram of a two-stage pulse in UO_2 : the sample is first heated at a preconditioning temperature of 3050 K and then submitted to a rapid pulse up to above the melting point. The freezing plateau (enlarged in the inset) is, in this case, long and very well defined.

for this type of rapid energy injection, the ascending flank of the thermogram does not present a clear thermal arrest at the melting point, while during cool-down, due to the ongoing steady-state heating, the thermal arrest plateau is very flat and has a comparatively long duration. The measured freezing point was stable within 5 K for almost 60 ms, and the reproducibility of the brightness temperature on freezing was ± 10 K. Considering the uncertainty in the emissivity, the melting temperature is $T_m(1 \text{ bar}) = 3130 \pm 20$ K.

With the present device, only single pulses, starting from room temperature, could be used for measurements at high pressure. In order to check whether the pulse heating presented regular features, calculations were made with a computer code simulating the heat propagation in the sample. The results generally show that the predicted peak temperature and the length of the freezing plateau are in agreement with the experimental data.

The variation of the measured melting point with pressure is plotted in Fig. 4. The three solid lines across the experimental points represent, respectively, the linear interpolation line (regression coefficient = 0.92) and the probable error band, while the two dotted lines indicate the 95% prediction band. The average slope of the melting line is $41 \text{ K} \cdot \text{kbar}^{-1}$, almost four times larger than that in tungsten. In order to ascertain that

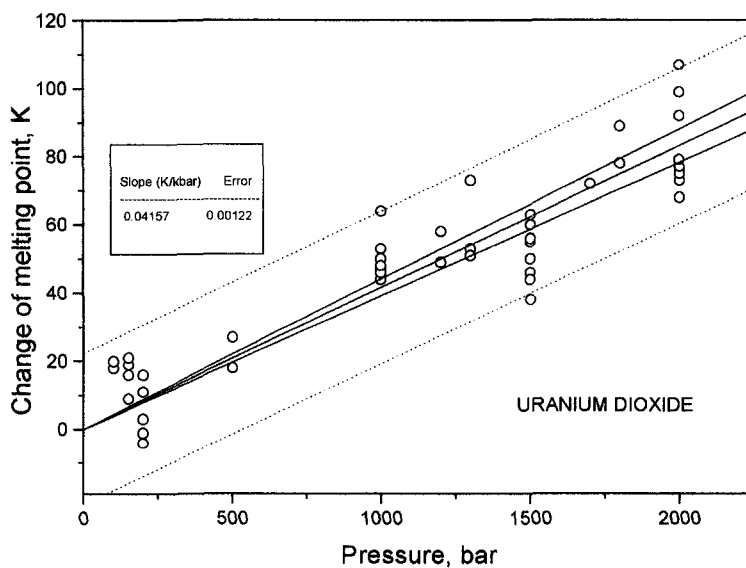


Fig. 4. Melting point increase as a function of pressure in UO_2 . The temperature variations were calculated by assuming the melting point at 1 bar to be equal to 3120 K. The thick line represents the linear regression curve, which was constrained to pass through zero; the two adjacent lines define the probable error band, and the dashed curves the 95% prediction band of the local measurements. The fitting parameters are given in the legend.

this variation was *not* due to stoichiometric changes of $\text{UO}_{2.00}$, the samples were submitted to measurement cycling over the complete pressure range; no hysteresis effects were detected, the measured melting points being well reproducible.

3.2. Tungsten

The melting temperature of tungsten measured at room pressure is 3680 ± 10 K, whereby the reproducibility of the brightness temperature on the freezing plateau is ± 6 K. The pressure dependence of T_m for tungsten is plotted in Fig. 5. The lines in the graph have the same meaning as in Fig. 4. The slope in this case is $9 \text{ K} \cdot \text{kbar}^{-1}$, with a regression coefficient of the interpolation straight line somewhat worse than in the case of UO_2 . The observed increase in the melting temperature between 10 and 2000 bar is approximately 30 K, i.e., five times the measurement precision.

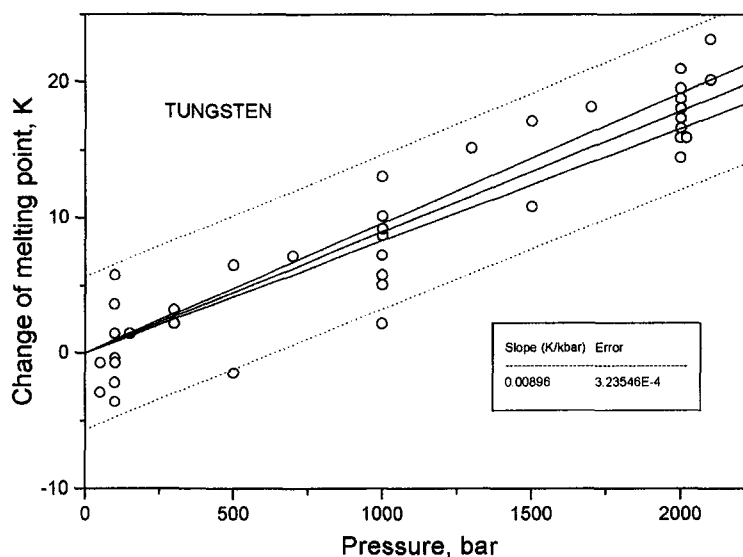


Fig. 5. Increase in tungsten melting point as a function of pressure. For the meaning of the plotted lines, see the legend to Fig. 4. The melting point at 1 bar was here assumed to be 3685 K.

3.3. Graphite

The melting point of graphite could be detected only at pressures above 110 bar. Below this pressure no stable liquid formation could be observed. Only at higher pressures was a thermal arrest clearly detected at a temperature of 4800 ± 150 K. The measurement of the melting point of graphite was particularly difficult, because of the high temperature involved and of the large vaporization rate of graphite at temperatures above melting. Therefore, the higher the pressure, the better was the reproducibility of the results. It should be noted that the measured T_m at 110 bar falls, within the error band, on the equilibrium vapor pressure curve of graphite. This should confirm that the triple point of graphite/liquid/vapor is (4800 K, 110 bar).

Figure 6 shows the values obtained at the different pressures; in this graph, unpublished measurements have been also plotted (filled triangles), which were obtained with a more complex autoclave, where a spherical sample was heated by four laser beams. Although the scatter is very large, an increase in the melting point with pressure can be deduced, with a slope of the order of $10 \text{ K} \cdot \text{kbar}^{-1}$.

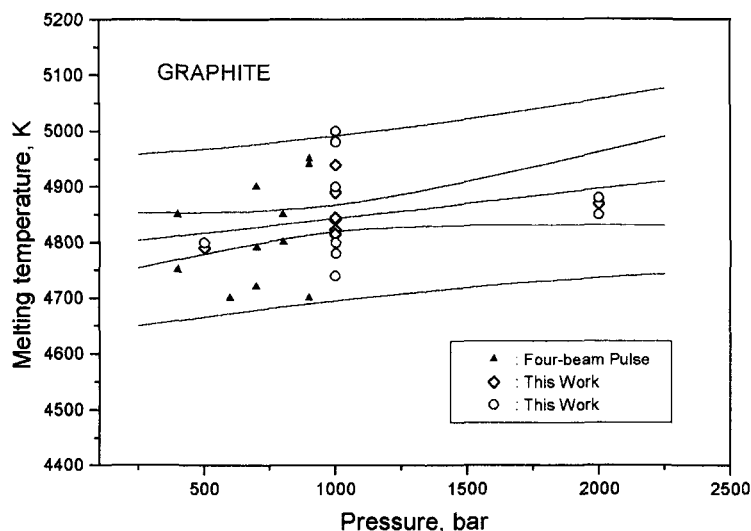


Fig. 6. Melting point of graphite as a function of pressure. The meaning of the lines is as in the legend to Fig. 4.

4. DISCUSSION

The experimental data on the variation of the melting temperature with pressure (melting slope) can be compared with the values predicted by the Clausius–Clapeyron equation:

$$\frac{dT_m}{dp} = \frac{\Delta V_f}{\Delta S_f} \quad (1)$$

which asserts that, under equilibrium conditions of liquid and solid, the rate of variation of T_m with pressure must be equal to the ratio of the volume change on melting to the entropy of fusion. The right-hand side of Eq. (1) can be evaluated from existing thermodynamic data, which are reported in Table I.

In the case of tungsten, the simplest among the materials examined, one can see from Table I that the thermodynamic data, especially for expansion on melting, are very uncertain. If these data are substituted into Eq. (1), they give melting slopes which are lower than those measured in our experiment, with a discrepancy much larger than our experimental error. On the other hand, it is unlikely that this discrepancy is due solely to an underevaluation of the less precise expansion on melting, since the maximum reported value ($4.7 \text{ cm}^3 \cdot \text{kg}^{-1}$, i.e., $\Delta V_f/V_s \cong 8\%$) is relatively

Table I. Thermochemical Data Used for Calculation of the Melting Slope

	T_m (K)	Ref. No.	$\Delta H^f(a, b)$ (MJ · kg ⁻¹)	$\Delta V_f(a, b)$ (m ³ · kg ⁻¹)	dT/dp (K · kbar ⁻¹)	
					Eq. (1)	Exp.
Tungsten	3680	5	0.30	1.5×10^{-6}	1.8	
		6	0.26	4.7×10^{-6}	6.6	9.0
		7	0.19	—	9.0	
		8	—	—	17.0	
Uranium dioxide	3130	9	0.29	11×10^{-6}	11.0	41.0
Graphite	4800	10	8.3	240×10^{-6}	15.0	≈ 10.0

large for a metal. Better agreement is obtained if old measurements of the enthalpy of melting ($\cong 1.9 \text{ MJ} \cdot \text{kg}^{-1}$) are used, though these should be less precise than those presently recommended, which give an entropy of fusion of $\cong 1.5$ i.e., a value quite in line with those of the other fcc metals. It should, however, be remarked that a detailed, comparative study of the equation of state of various metals conducted by Glasow [8], predicts a melting slope of $17 \text{ K} \cdot \text{kbar}^{-1}$ for tungsten, i.e., higher than our experimental value. It, therefore, cannot be excluded that the melting slope calculated from Eq. (1) is affected by errors in the presently recommended thermochemical data.

The results for UO_2 are more problematic. There is, in fact, no way of explaining the large difference between the calculated and the measured melting slopes. The measured melting temperature increase between 1 and 2000 bar is too large and accurate for attempting any compensation in terms of possible experimental uncertainties of the data. We must, therefore, admit that Eq. (1) is not satisfied in the case of uranium dioxide.

Actually, since UO_2 is a complex substance (one is not even sure that it melts congruently at our composition), one can argue that, if during the applied pulses solid and liquid UO_2 were not in thermodynamic equilibrium, Clapeyron's equation in the form of Eq. (1) is not applicable. This could explain the occurrence of a deviation from the equilibrium melting slope; it remains, however, unclear, which process could affect the entropy of the liquid (or of the solid) to such an extent as to produce the large pressure dependence of the melting point observed in our experiment.

A modification of the setup is in progress, with the aim of enabling two-stage pulses (such as that shown in Fig. 3) to be applied also at high pressures. We hope that the analysis of detailed, longer freezing plateaus will produce new evidence on the nature of the melting transition at different pressures.

Finally, the minimum pressure (110 bar) at which the melting point of graphite could be measured (4800 K) is very near the equilibrium vapor pressure at the same temperature. This means that 110 bar (4800 K) indeed represents the triple point, below whose coordinates graphite cannot be melted under equilibrium conditions.

Furthermore, in spite of the greater experimental difficulties and the lower precision of the temperature measurements, the results for graphite essentially show reasonable agreement with the predictions of Eq. (1). In fact, the large expansion on melting observed ($\cong 45\%$) compensates for the high fusion enthalpy (and entropy) of graphite, so that a melting slope of the order of $10 \text{ K} \cdot \text{kbar}^{-1}$ is predicted, which is effectively confirmed by our data. Therefore, these results provide an independent proof of the consistency of the thermodynamic melting data of graphite.

ACKNOWLEDGMENT

This study was conducted with the support of the International Association for the promotion of cooperation with scientists from the New Independent States of the former Soviet Union (INTAS).

REFERENCES

1. L. F. Vereshchagin and N. Fateeva, *High Temp.-High Press.* 9:619 (1977).
2. M. Sheindlin, *Sov. Tech. Rev. B Therm. Phys.* 4:1 (1992).
3. M. Bober and J. Singer, *Nucl. Sci. Eng.* 97:344 (1987).
4. J. P. Hiernaut, F. Sakuma, and C. Ronchi, *High Temp.-High Press.* 21:139 (1989).
5. R. S. Hixson and M. A. Winckler, *Int. J. Thermophys.* 11:709 (1990).
6. A. Berthault, L. Arles, and J. Matricon, *Int. J. Thermophys.* 7:167 (1986).
7. C. Robert (ed.), *Handbook of Chemistry and Physics* (Academic Press, New York, 1979/1970), p. 196.
8. V. M. Glasow, V. S. Lasarev, and V. V. Zhakov, *Phase Diagrams of Simple Substances* (Izdatel'stvo Nauka, Moscow, 1980), p. 149.
9. J. K. Fink and M. C. Petri, Report ANL/RE-97/2 (Argonne Natl. Lab., Argonne, IL, 1997).
10. L. V. Gurvich and V. S. Iorish, *Database IVTANTHERMO* (Thermocenter RAS, 1993).